

# Phosphene Evaluation in a Visual Prosthesis with Artificial Neural Networks

Cédric Archambeau<sup>1</sup>, Amaury Lendasse<sup>2</sup>, Charles Trullemans<sup>1</sup>, Claude Veraart<sup>3</sup>, Jean Delbeke<sup>3</sup>, Michel Verleysen<sup>1,\*</sup>

<sup>1</sup> Université Catholique de Louvain – Laboratoire de micro-électronique  
Place du Levant 3, B-1348 Louvain-la-Neuve, Belgium  
Phone: +32-10-47-25-40, Fax: +32-10-47-25-98  
email: {archambeau,ctrullemans,verleysen}@dice.ucl.ac.be

<sup>2</sup> Université Catholique de Louvain – CESAME  
avenue G. Lemaître 4, B-1348 Louvain-la-Neuve, Belgium  
Phone: +32-10-47- 80-46, Fax: +32-10-47-21-80  
email: lendasse@auto.ucl.ac.be

<sup>3</sup> Université Catholique de Louvain – Laboratoire de Génie de Réhabilitation Neurale  
avenue Hippocrate 54, B-1200 Bruxelles, Belgium  
Phone: +32-2-764-95-77, Fax: +32-2-764-94-22  
Email: {delbeke,veraart}@gren.ucl.ac.be

**ABSTRACT:** The electrical stimulation of the optic nerve is investigated, as an approach to the development of a microsystems-based visual prosthesis. Non-linear prediction models, i.e. artificial neural networks, for phosphene localisation are used and show promising results. The prediction error is reduced up to 20% in comparison with linear statistical models and the error standard deviation is restrained such that the prediction accuracy is similar to the measurements accuracy. In addition, it is shown that linear methods do not suit this kind of problems.

**KEYWORDS:** Rehabilitation, optic nerve, electrical stimulation, artificial neural networks, cross-validation.

## INTRODUCTION

Recently, it has been shown that electrical stimulation of the optic nerve is possible on blind patients suffering from retinitis pigmentosa (RP) [1]. The principle relies on the selective response of the human optic nerve to adequately chosen electrical pulses. The main parameters of the pulses are shape, duration, frequency, amplitude and number of pulse repetitions. The selectively stimulated sections of the optic nerve will in turn produce phosphenes at different locations in the visual field of the patient. Those can also be characterized by their colour, shape and intensity.

An electronic system aimed at capturing images and transforming them into electrical stimulations applied to the optic nerve has been realized [2]. The system includes an artificial retina, an external device that processes the image and codes it into a restricted data stream, a transcutaneous link forwarding the data, the power supply and the clock to an internal circuit, which in turns decodes the data stream into waveforms applied to the optic nerve through a cuff electrode with four contacts wrapped around it.

The electrode has been implanted on a volunteer and a number of experiments have been conducted in order to establish the characteristics of the generated phosphenes with respect to the stimulating parameters [3]. These experiments were aiming at the study of perception thresholds, as well as phosphene temporal and spatial summation mechanism and the

---

\* Michel Verleysen is a Research Associate of the Belgian F.N.R.S. (National Fund for Scientific Research).

The development of a visual prosthesis is a project funded by the European Commission (Esprit LTR 22527 "Mivip" and IST-2000-25145 "Optivip" grants), and by the Belgian Fund for Medical Scientific Research (grant # 3.4584.98).

relationship between the stimulation parameters and the characteristics of the phosphenes. In this paper we will focus on the prediction of the position of the phosphenes.

The complexity of the physiologic process, whereby the electrical pulses applied to the optic nerve generate phosphenes, makes it difficult to study it on a biological level. Furthermore, it must be stressed that the optic nerve of RP patients is probably damaged up to some unknown degree. Finally, the characteristics of the phosphenes correspond to description by a blind volunteer of subjective perceptions, clearly subject to human inaccuracies and errors. For these reasons, a mathematical identification of the process is better suited in order to obtain a model that can be used to predict the stimulation results, plan efficiently new tests and, as a long-term goal, derive algorithms, which will be used to transform an incoming image into an adequate set of electrical pulses and give rise to a well reconstructed image.

As linearity of the whole process cannot be expected, non-linear models, i.e. artificial neural networks, are preferred. In addition, the adaptation abilities of neural networks allow us to build a model that evolves as information from new experiments is gained. Furthermore, we expect, in the future, to obtain different, but similar models for other patients. The global structure of the model, for example the number of nodes, found with one patient may be expected to be appropriate for new ones.

Subsequently we will first recall the principles of a linear regression, as well as the principles of RBFN (*radial-basis function net*) and MLP (*multi-layer perceptron*), which are non-linear data prediction models. Secondly, we will present an optimisation strategy of those neural networks based on cross-validation. Finally, we will show that the use of non-linear models to identify the relation between stimulation parameters and phosphene characteristics have shown improved performances with respect to traditional linear statistical analysis. Indeed, the prediction root mean square error (RMSE), for example, was reduced by a quantity up to 20%.

## DATA PREDICTION MODELS

A preliminary work consisted of the data-acquisition. Single current pulse trains are injected to the optic nerve of the blind volunteer via the cuff electrode. The input parameters considered are pulse duration, number of pulses, amplitude and frequency, while the chosen output parameters are the horizontal and vertical position of the phosphenes. Both directions are supposed independent and thus the neural networks for both outputs were trained separately.

The network training can be decomposed in two steps: the learning and the generalization. Hence, the aim of network training is not to learn an exact representation of the training data itself, but rather to build a statistical model of the process that generates the data, such that it achieves a good prediction model for new inputs.

In this section we are reviewing several types of artificial neural networks. The first one is the linear type and the second and third one are both non-linear methods. The linear method is exposed as reference, to validate the approximation improvement achieved by the non-linear ones.

### LINEAR REGRESSION

A linear regression with five inputs can be defined as follows:

$$y_k^{(i)} = \sum_j^5 w_{k,j} x_j^{(i)}, \quad i = 1, 2, \dots, N_t. \quad (1)$$

In this equation  $N_t$  is the number of training data and the input vector  $\mathbf{x}^{(i)}$  contains the four parameters considered: duration, current intensity, number of pulses and frequency. In addition, one extra element was concatenated to each input vector for the bias, which represents the independent term in the model. The output  $y_k^{(i)}$  can be either the position in the horizontal or the vertical direction ( $k = H, V$  respectively); to each one corresponds a weight vector  $\mathbf{w}_k$ .

### MULTI-LAYER PERCEPTRON

Linear regressions can be considered as non-adaptive single-layer networks, which can be extended to multiple-layer networks. Whereas single-layer networks have limited applications, MLPs have the universal approximation property and, therefore, they can approach any kind of process provided the network contains a sufficient number of parameters.

Since a restricted number of layers reduces the complexity as well as the training period, a minimum number of layers is suitable.

The equation of a 2-layer perceptron can be written as follows [4]:

$$y_k^{(i)} = h \left( \sum_l^Q w_{k,l}^{(2)} \cdot g \left( \sum_j^5 w_{k,lj}^{(1)} x_j^{(i)} \right) \right), \quad i = 1, 2, \dots, N_t \quad (2)$$

where  $h(\cdot)$  and  $g(\cdot)$  are so-called activation functions. The superscript of the weight matrix corresponds to the layer of the network and  $Q$  is the number of nodes. The activation function of the output units,  $h(\cdot)$ , is chosen, in our case, as the identity function and thus, avoids saturation of the outputs; the internal one,  $g(\cdot)$ , is a sigmoidal function.

The learning for a MLP consists of finding a set of parameters  $w_{k,lj}^{(1)}$  and  $w_{k,l}^{(2)}$  such that equation (2) holds as far as possible, for all known input-output pairs of the process we are trying to approximate. In other words, we are minimizing an error criterion, usually defined as the mean square error:

$$MSE_k = \frac{1}{N_t} \sum_i^{N_t} (d_k^{(i)} - y_k^{(i)})^2, \quad (3)$$

where  $d_k^{(i)}$  are the desired outputs and  $y_k^{(i)}$  are the approximated outputs.

## RADIAL BASIS FUNCTION NETWORK

While a MLP approximates any type of function by combining sigmoids, a RBFN approximates functions by a combination of radial basis functions. The universal approximation property holds for RBFN as well.

The training of a RBFN is subdivided in two steps. The first one is unsupervised. It consists of choosing the centers  $\mathbf{c}_{k,j}$ , named centroids, of the radial basis function by a vector quantization method and calculating their standard deviation  $\sigma_{k,j}$ . The vector quantization method we have opted for is a competitive learning scheme (see for example [5]). The second step consists of a supervised approximation of the outputs by a set of  $P$  basis function  $\varphi(\cdot)$  [4]:

$$y_k^{(i)} = \sum_j^P w_{k,j} \varphi(\|\mathbf{x}^{(i)} - \mathbf{c}_{k,j}\|). \quad (4)$$

The most commonly used type of basis function is the Gaussian :

$$\varphi(\|\mathbf{x}^{(i)} - \mathbf{c}_{k,j}\|) = \exp \left( - \frac{\|\mathbf{x}^{(i)} - \mathbf{c}_{k,j}\|^2}{2 \cdot \gamma_k \cdot \sigma_{k,j}} \right), \quad (5)$$

where  $\gamma_k$  is an adaptation factor. The parameter  $\gamma_k$  is added to give more flexibility to the approximation function (4). Indeed, there is no reason that choosing  $\gamma_k = 1$  is the best choice (in terms of approximation error); learning  $\gamma_k$  as parameter allows to further optimise the network in order to increase the approximation quality [6].

The learning for RBFN turns out to be analogous as for the MLP, except that the set of parameters to find are the centroids  $\mathbf{c}_{k,j}$ , the standard deviations  $\sigma_{k,j}$  and the factors  $w_{k,j}$ .

## CROSS-VALIDATION

In this section we are going to outline our strategy to tune the parameters of the approximation networks. First of all the data is randomly split in a training data set and a validation data set, which contain respectively 80% and 20% of the original data set. Then, various networks are trained on the training sets. Finally, the performance of the networks is estimated by minimizing an appropriate error function evaluated with respect to the validation sets.

If this procedure is repeated several times, using different training and validation data sets, optimal parameters can be found by averaging the error. The parameters that were optimised according to this method are the number sigmoids for the 2-layer MLP and the number of Gaussian functions, as well as parameter  $\gamma_k$  for the RBFN.

## EXPERIMENTAL RESULTS

Let us define, for convenience, the root mean square error:

$$RMSE_k = \sqrt{\frac{1}{N_v} \sum_i^{N_v} (d_k^{(i)} - y_k^{(i)})^2}, \quad (6)$$

where  $N_v$  is the number of validation data.

Consider the MLP network exposed previously. An optimal number of nodes has to be determined in order to approximate the process accurately while avoiding overfitting and thus bad generalization. Overfitting is the phenomenon encountered when the network fits so perfectly the training data that it performs badly on any other set of data, as for example the validation data. The error functions with respect to the number of nodes are plotted in Figure 1. Note that the data were normalized. Moreover, it should be stressed that some results were left out: in some cases the MLP did not converge properly and reached a local minimum; as a consequence the MSE was not representative of the performance that could be achieved by the MLP.

On the other hand, for the RBFN we have to find the optimal number of centroids for the vector quantization and an optimal value for the parameter  $\gamma_k$ . The error in function of those two parameters is shown in Figure 2. Observe that for the RBFN no convergence problem was noted. One can also notice that, in contradiction with the MLP, the error does not increase after a certain number of centroids. This can be explained by the fact that when too many centroids are used, their corresponding radial basis function are set to merely zero. A good choice for the number of centroids is the number corresponding to the end of the elbow, since a further increase would not improve significantly the quality, whereas the complexity would grow drastically.

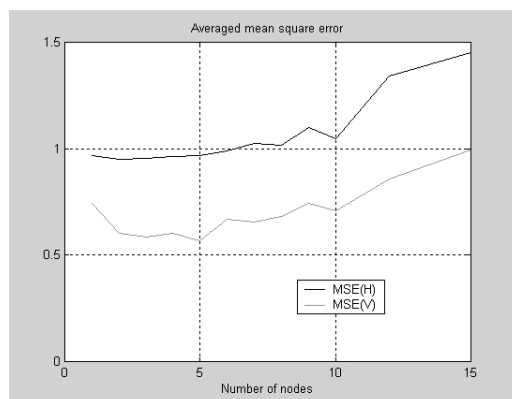


Figure 1: MSE in the horizontal and vertical direction for the third electrode contact (180°) and 150 cross-validations.

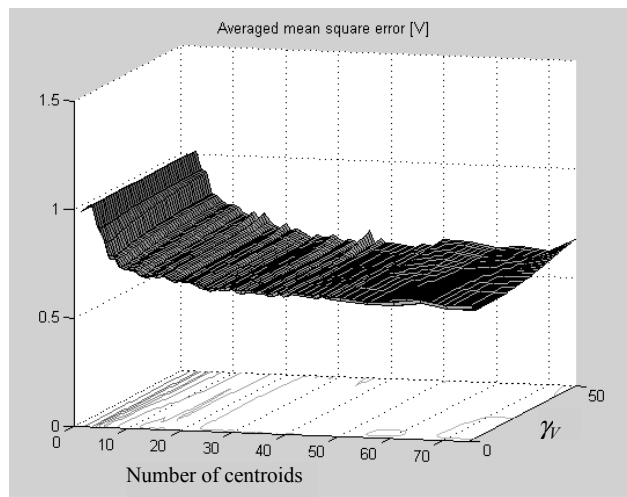


Figure 2: MSE in the vertical direction for the third electrode contact (180°), 150 cross-validation and  $\gamma_k = 1,2 \dots 50$ .

For the MLP as well as for the RBFN, the error in the vertical direction is lower than in the horizontal direction, for all electrode contacts. This is probably due to the fact that the observed range of phosphene positions was much larger in the vertical than in the horizontal direction, thus yielding corresponding relative inaccuracies.

The RMSE values obtained for each contact, using denormalized data, are presented in Table I. The linear model shows very little prediction capabilities since the approximation error and the standard deviation, in both directions, are of the same order (see Table II). We see in Table I that the non-linear data prediction models reduce the approximation error by about 10% in the horizontal direction and about 20% in the vertical direction.

Finally we can investigate the distribution of the approximation error. The error distribution of the linear regression, the MLP and the RBFN are plotted respectively in Figure 3, Figure 4 and Figure 5. Note that the error distribution of the two non-linear methods is approximately Gaussian.

|          | Contact 0° |       | Contact 90° |       | Contact 180° |       | Contact 270° |      |
|----------|------------|-------|-------------|-------|--------------|-------|--------------|------|
|          | H          | V     | H           | V     | H            | V     | H            | V    |
| LIN.REG. | 4.6°       | 14.0° | 5.4°        | 14.8° | 6.2°         | 14.9° | 6.1°         | 9.4° |
| MLP      | 4.3°       | 11.7° | 5.0°        | 12.4° | 5.8°         | 12.3° | 5.5°         | 9.3° |
| RBFN     | 4.2°       | 11.8° | 4.9°        | 12.6° | 5.7°         | 11.8° | 5.4°         | 8.2° |

Table I.: RMSE for each contact.

|      | Contact 0° |        | Contact 90° |       | Contact 180° |        | Contact 270° |      |
|------|------------|--------|-------------|-------|--------------|--------|--------------|------|
|      | H          | V      | H           | V     | H            | V      | H            | V    |
| MEAN | 3.9°       | -5.34° | 4.7°        | -9.2° | 0.2°         | -12.5° | -4.6°        | 4.1° |
| STD  | 4.5°       | 14.2°  | 5.2°        | 17.6° | 6.1°         | 15.4°  | 6.1°         | 9.3° |

Table II.: Mean and Standard deviation of the data for each contact.

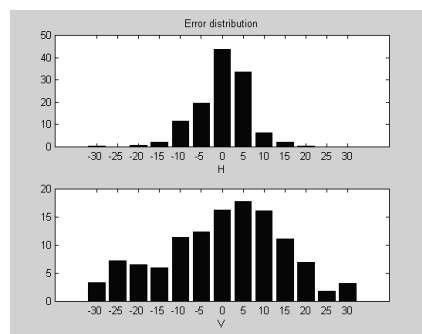


Figure 3: Error distribution after approximation by a linear regression for contact 180° [ $\sigma_H=6.2^\circ$ ,  $\sigma_V=14.8^\circ$ ].

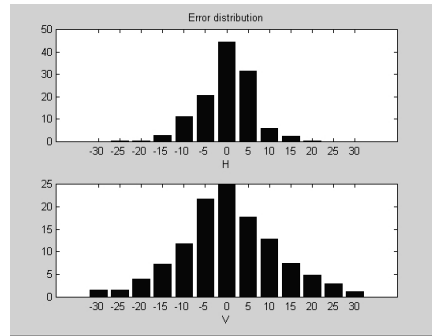


Figure 4: Error distribution after approximation by a MLP for contact 180° [ $\sigma_H=6.1^\circ$ ,  $\sigma_V=12.8^\circ$ ].

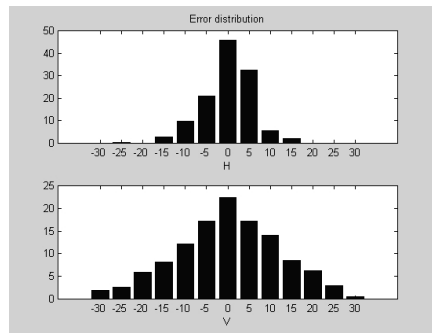


Figure 5: Error distribution after approximation by a RBFN for contact 180° [ $\sigma_H=5.6^\circ$ ,  $\sigma_V=11.9^\circ$ ].

## CONCLUSIONS

The purpose of this work is to show that the position of phosphenes could be predicted with a satisfactory precision, using data gained in a research project about visual rehabilitation by electrical stimulation of the optic nerve.

At first sight, the results in Table I might be considered as poor, since the RMSE is of the same order of magnitude as the standard deviation. Nevertheless, a closer look to Figure 4 and Figure 5 shows that the errors are mostly localised in a short interval around zero and that an accuracy of about 5° in horizontal direction and 10° in vertical direction can be expected for the whole process. Remembering that the values to approximate are resulting from human response, which is definitely not accurate, we conclude on satisfactory results.

Moreover, the comparison between Figure 3 and the Figures 4 or 5 shows that a clear prediction improvement is obtained by non-linear models with respect to the linear regression. It should be stressed that the prediction accuracy achieved by those methods is of the same order of magnitude as the precision of the measurements. A linear model is therefore not suited to predict phosphene localisation in the visual field. One can also note that the improvement seems to be better in the vertical direction, since the reduction of the standard deviation is greater in that particular direction. This is probably due to the fact that the optic nerve is more damaged in the horizontal direction, which resulted in an increased inaccuracy of the human response.

Finally, it should be noted that the performance of the RBFN is better than the performance of the MLP. Indeed, despite the fact that the error reduction is of the same order for both methods, the standard deviation of the RBFN error is significantly lower, which proves a greater prediction accuracy. In addition, for the RBFN no convergence problems arose.

## REFERENCES

- [1] C. Veraart, C. Raftopoulos, J.T. Mortimer, J. Delbeke, D. Pins, G. Michaux, A. Vanlierde, S. Parrini and M.C. Wanet-Defalque, 1998, "Visual sensations produced by optic nerve stimulation using an implanted self-sizing spiral cuff electrode", *Brain Research*, vol. 813 pp. 181-186.
- [2] P. Doguet, H. Mevel, M. Verleysen, M. Troosters, C. Trullemans, 2000, "An integrated circuit for the electrical stimulation of the optic nerve", *IFESS'2000*, Aalborg, Denmark, 18-19 June 2000, pp. 18-20.
- [3] J. Delbeke, S. Parrini, O. Glineur et al., 1999, "Phosphene perception thresholds to direct stimulation of a human optic nerve shows spatial and temporal summation", 29<sup>th</sup> Ann. Meeting Soc. For Neuroscience, Miami, USA, 23-28 October 1999.
- [4] C.M. Bishop, 1995, "Neural Networks for Pattern Recognition", Clarendon Press, Oxford.
- [5] T. Kohonen, 1995, "Self-organizing maps", Springer, Berlin.
- [6] M. Verleysen, K. Hlavackova, 1994, "An optimised RBF network for approximation of functions", *European Symposium on Artificial Neural Networks*, Brussels, Belgium, April 1994.